

A one-phase Stefan problem with size-dependent thermal conductivity

F. Font

Department of Physics, Universitat Politècnica de Catalunya, Barcelona, Spain

December 3, 2024

Abstract

In this paper a one-phase Stefan problem with size-dependent thermal conductivity is analysed. Approximate solutions to the problem are found via perturbation and numerical methods, and compared to the Neumann solution for the equivalent Stefan problem with constant conductivity. We find that the size-dependant thermal conductivity, relevant in the context of solidification at the nanoscale, acts to slow down the solidification process. Interestingly, a small time asymptotic analysis reveals that the position of the solidification front in this regime behaves linearly with time, in contrast to the Neumann solution characterized by a square root of time proportionality. This has an important physical consequence, namely the speed of the front predicted by size-dependant conductivity model is finite while the Neumann solution predicts an infinite and, thus, unrealistic speed as $t \rightarrow 0$.

1 Introduction

The Stefan problem, describing the phase change of a material, is one of the most popular in the literature of moving boundary problems. It requires solving heat equations for the two phases (*e.g.* solid and liquid), while the position of the front separating them, the moving boundary, is determined from an energy balance, referred to as the Stefan condition. The Stefan problem has been studied in great detail since Lamé and Clapeyron wrote it down for the first time in the 19th century. There are several reference books that the reader is referred to for a comprehensive background on the classical problem [12, 7, 4, 8, 1, 13]. The problem only admits an exact solution in the Cartesian one-dimensional case, which receives the name of Neumann solution (see, for instance, [13]). Solutions in

other geometries or extra dimensions are usually found numerically or by means of asymptotic/perturbation techniques [14, 10].

The classical problem has been modified in quite different ways to introduce new physical phenomena such as supercooling or curvature dependent phase change temperature [6, 5, 3]. Modifications are usually linked with a thermophysical property of the material which in fact appears to change with, for example, the geometry of the system (*e.g.* curvature-induced melting point depression), the speed of the moving boundary (*e.g.* supercooling), or the temperature itself. Heat conduction experiments on Silicon nanowires have shown that the thermal conductivity decreases when the system of the system decreases, thus providing a new example where the value of a thermophysical property depends on the size of the physical system. In Jou et al [9] the following analytical expression for the dependence on the size of the system of the thermal conductivity of a solid is derived

$$k = \frac{2k_0 L^2}{l^2} \left(\sqrt{1 + \frac{l^2}{L^2}} - 1 \right), \quad (1)$$

where k_0 represents the bulk thermal conductivity of the solid, L the size of the solid, l phonon mean free path. In a later paper, the authors compare expression (1) with experimental data showing good agreement [2]. The main goal of this letter is to study the effect of the size-dependent thermal conductivity (1) in the solution of the Stefan problem.

The rest of the paper is organized as follows. In the next section we formulate the Stefan problem with size dependent thermal conductivity and discuss how the Neumann solution can be retrieved. In section 3 we provide a perturbation solution based on large Stefan number. In section 4 we explain a numerical strategy and analyse the small time limit, which is needed to initialize the numerical code. In section 5 we discuss our results and in section 6 we draw our conclusions.

2 Problem formulation

Consider a liquid initially at the equilibrium freezing temperature, T_f , occupying the space $x \geq 0$. Suddenly, the temperature is lowered to $T_c < T_f$ on the edge $x = 0$ and the liquid starts to solidify. The newly created solid phase will start to grow occupying the space $0 < x < s(t)$, where $s(t)$ represents the position of the solidification front as well as the size of the whole solid phase. Then, finding the temperature of the solid phase, $T(x, t)$, will require solving the governing equation

$$\rho c \frac{\partial T}{\partial t} = k(s(t)) \frac{\partial^2 T}{\partial z^2} \quad \text{on} \quad 0 < z < s(t), \quad (2)$$

ρ (kg/m ³)	c (J/kg·K)	k_0 (W/m·K)	T_f K	ΔH (J/kg)	l (m)
2320	770	120	1687	1926×10^3	40×10^{-9}

Table 1: Thermophysical properties of Silicon.

where ρ is the density, c the specific heat, and $k(s(t))$ the thermal conductivity which depends on the size of the solid phase and is obtained by setting $L = s(t)$ in (1). That is,

$$k(s(t)) = \frac{2k_0 s(t)^2}{l^2} \left(\sqrt{1 + \frac{l^2}{s(t)^2}} - 1 \right). \quad (3)$$

Note, the liquid phase will remain at T_f and no equation is needed for the temperature of the liquid. The temperature of the solid will be subject to the boundary conditions

$$T(0, t) = T_c, \quad T(s(t), t) = T_f. \quad (4)$$

Finally, at the solidification front we have the Stefan condition that will be employed to determine $s(t)$

$$\rho \Delta H \frac{ds}{dt} = k(s(t)) \left. \frac{\partial T}{\partial z} \right|_{z=s(t)}, \quad (5)$$

where ΔH is the latent heat of fusion. In what follows, we will use as a reference the parameter values for Silicon indicated in Table 1.

2.1 Nondimensional model

Introducing the nondimensional variables

$$\hat{T} = \frac{T - T_f}{T_f - T_c}, \quad \hat{x} = \frac{x}{\Lambda}, \quad \hat{t} = \frac{t}{\mathcal{T}}, \quad \hat{s} = \frac{s}{\Lambda},$$

in (2)-(5) and taking the scales $\Lambda = l$ and $\mathcal{T} = \Lambda^2 c \rho / k$, we obtain the dimensionless model

$$\frac{\partial T}{\partial t} = 2s \left(\sqrt{s^2 + 1} - s \right) \frac{\partial^2 T}{\partial z^2} \quad \text{on} \quad 0 < z < s(t), \quad (6a)$$

$$T(0, t) = -1, \quad (6b)$$

$$T(s(t), t) = 0, \quad (6c)$$

$$\beta \frac{ds}{dt} = 2s \left(\sqrt{s^2 + 1} - s \right) \left. \frac{\partial T}{\partial z} \right|_{z=s}, \quad (6d)$$

$$s(0) = 0, \quad (6e)$$

where $\beta = \Delta H/c\rho$ is the Stefan number. It can be shown how $2s(\sqrt{s^2+1}-s) \rightarrow 1$ when $s(t) \rightarrow \infty$, retrieving the classical case.

2.2 Neumann solution

The classical one-phase Stefan problem can be retrieved by setting the size-dependent thermal conductivity, $k = 2s(\sqrt{s^2+1}-s)$, in (6a) and (6e) to 1. In this case, the problem has exact solution, which can be found by reducing the heat equation (6a) using the similarity variable $\eta = x/\sqrt{t}$ into the ordinary differential equation $-\frac{\eta}{2}T_\eta = T_{\eta\eta}$. The equation can be solved in terms of the error function to give

$$T(x, t) = -1 + \frac{\operatorname{erf}\left(\frac{x}{2\sqrt{t}}\right)}{\operatorname{erf}(\lambda)}, \quad (7)$$

and the solution for $s(t)$ is found by substituting (7) into the Stefan condition, which results in

$$s(t) = 2\lambda\sqrt{t}, \quad \beta\sqrt{\pi}\lambda \operatorname{erf}(\lambda) e^{\lambda^2} = 1. \quad (8)$$

The set (7)-(8) receives the name of Neumann solution.

3 Perturbation solution

The complexity introduced by the size dependent thermal conductivity in the governing equation prevents an exact similarity solution as in the classical SP. In order to find an approximate analytical solution, we make use of a standard perturbation technique. We consider β to be large for our system (for instance, for $\Delta T = 130\text{K}$ we have $\beta \approx 20$) and rescale time as $t = \beta\hat{t}$. Defining the small parameter $\delta = \beta^{-1}$, the problem becomes

$$\delta \frac{\partial T}{\partial \hat{t}} = 2s(\sqrt{s^2+1}-s) \frac{\partial^2 T}{\partial z^2}, \quad (9a)$$

$$T(0, \hat{t}) = -1, \quad (9b)$$

$$T(s(\hat{t}), \hat{t}) = 0, \quad (9c)$$

$$\frac{ds}{d\hat{t}} = 2s(\sqrt{s^2+1}-s) \left. \frac{\partial T}{\partial z} \right|_{z=s}, \quad (9d)$$

$$s(0) = 0, \quad (9e)$$

suggesting an expansion in the form $T(x, \hat{t}) = T_0 + \delta T_1 + \mathcal{O}(\delta^2)$. We obtain the leading and first order problems

$$\mathcal{O}(1) : \quad 0 = \frac{\partial^2 T_0}{\partial z^2}, \quad T_0(1, \hat{t}) = -1, \quad T_0(s(\hat{t}), \hat{t}) = 0, \quad (10)$$

$$\mathcal{O}(\delta) : \quad \frac{\partial T_0}{\partial \hat{t}} = 2s \left(\sqrt{s^2 + 1} - s \right) \frac{\partial^2 T_1}{\partial z^2}, \quad T_1(1, \hat{t}) = 0, \quad T_1(s(\hat{t}), \hat{t}) = 0, \quad (11)$$

with solutions

$$T_0 = -1 + \frac{x}{s}, \quad T_1 = \frac{s_{\hat{t}}}{12s^3 (\sqrt{s^2 + 1} - s)} x(s^2 - x^2). \quad (12)$$

These lead to the temperature profile

$$T(x, \hat{t}) = -1 + \frac{x}{s} + \frac{1}{\beta} \frac{s_{\hat{t}}}{12s^3 (\sqrt{s^2 + 1} - s)} x(s^2 - x^2) + \mathcal{O}(\delta^2). \quad (13)$$

Inserting $T \approx T_0 + \delta T_1$ into (9d) we obtain the following expression for the speed of the moving boundary

$$s_{\hat{t}} = \frac{6\beta}{(1 + 3\beta)} \left(\sqrt{s^2 + 1} - s \right), \quad (14)$$

which can be readily integrated and the initial condition (9e) applied to give

$$s^2 + s\sqrt{s^2 + 1} + \arcsin(s) = \frac{12\beta}{(1 + 3\beta)} \hat{t}. \quad (15)$$

4 Numerical solution

Coordinate transformations leading to the immobilization of moving boundaries are widely used when seeking numerical solution of moving boundary problems because of the advantage of working with fixed domains. In order to immobilise the boundary $s(t)$ we map the space variable x to the unit domain via the Landau-type transformation $\xi = x/s(t)$. Then, problem (6a)-(6e) becomes

$$s \frac{\partial T}{\partial t} = s_t \xi \frac{\partial T}{\partial \xi} + 2 \left(\sqrt{s^2 + 1} - s \right) \frac{\partial^2 T}{\partial \xi^2} \quad \text{on} \quad 0 < \xi < 1 \quad (16a)$$

$$T(0, t) = -1, \quad (16b)$$

$$T(1, t) = 0, \quad (16c)$$

$$\beta s_t = 2 \left(\sqrt{s^2 + 1} - s \right) \frac{\partial T}{\partial \xi} \Big|_{\xi=1}, \quad (16d)$$

$$s(0) = 0. \quad (16e)$$

A Backward Euler semi-implicit finite difference scheme may now be used on (16a), discretising implicitly for $T(\xi, t)$ and explicitly for $s(t)$ and $s_t(t)$, and using second order central differences in space. The semi-implicit scheme allows equation (16a) (containing time dependent coefficients) to be formulated, after discretising, as a matrix linear system which can be solved by inverting the matrix of the system at each time step. The position of the solidification front is found via (16d), using a backward difference for s_t and a one-sided second order difference for the partial derivative.

A typical issue in the numerical solution of Stefan problems is how to initiate the computation in a region which initially has zero thickness. A solvent approach to tackle this issue is to find a small time asymptotic approximation for T and s and input this as the initial condition in the numerical scheme [11]. We follow this approach which is detailed in the next section.

4.1 Small time limit

To study the small time limit we assume that $s(t)$ must be a power of time and match the initial condition $s(0) = 0$, so we set $s = \lambda_2 t^p$ where λ_2 and p are constants. Then, we rescale time as $t = \varepsilon\tau$, where $\varepsilon \ll 1$. Substituting the resulting expressions for the position and the velocity of the front, $s = \lambda_2 \varepsilon^p \tau^p$ and $s_t = p\lambda_2 \varepsilon^{p-1} \tau^{p-1}$, into (16d) we have

$$\frac{\beta}{2} p \lambda_2 \varepsilon^{p-1} \tau^{p-1} = \left(\sqrt{\varepsilon^{2p} \tau^{2p} + 1} - \lambda_2 \varepsilon^p \tau^p \right) \frac{\partial T}{\partial \xi} \Big|_{\xi=1}, \quad (17)$$

which, after multiplying the left hand side by $(\sqrt{\varepsilon^{2p} \tau^{2p} + 1} + \lambda_2 \varepsilon^p \tau^p)(\sqrt{\varepsilon^{2p} \tau^{2p} + 1} + \lambda_2 \varepsilon^p \tau^p)^{-1}$, and noting that $\sqrt{\varepsilon^{2p} \tau^{2p} + 1} \approx 1$ for $\varepsilon^{2p} \tau^{2p} \ll 1$, gives

$$\frac{\beta}{2} p \lambda_2 \varepsilon^{p-1} \tau^{p-1} (1 + \lambda_2 \varepsilon^p \tau^p) \approx \frac{\partial T}{\partial \xi} \Big|_{\xi=1}. \quad (18)$$

Now we need to choose p . We see that for the front to move the lhs in (18) must be $\mathcal{O}(1)$, thereby balancing the rhs. The balance is obtained for $p = 1$, so

$$s = \lambda_2 t, \quad (19)$$

for $t \rightarrow 0$. Substituting $s = \lambda_2 t$ in (16a) and taking the limit $t \rightarrow 0$ we get

$$0 = \xi \frac{\lambda_2}{2} \frac{\partial T}{\partial \xi} + \frac{\partial^2 T}{\partial \xi^2}, \quad (20)$$

with solution

$$T = -1 + \frac{\operatorname{erf}\left(\frac{\sqrt{\lambda_2}}{2}\xi\right)}{\operatorname{erf}\left(\frac{\sqrt{\lambda_2}}{2}\right)}. \quad (21)$$

Finally, the constant λ_2 is found by substituting (19) and (21) in (16d)c and taking the limit $t \rightarrow 0$, leading to the transcendental equation

$$\frac{\beta}{2}\sqrt{\pi}\sqrt{\lambda_2}\operatorname{erf}\left(\frac{1}{2}\sqrt{\lambda_2}\right)e^{\lambda_2/4} = 1. \quad (22)$$

From the physical standpoint expression (19) is quite interesting as it tells that the speed of the solidification front, s_t , is constant as $t \rightarrow 0$, in contrast to the Neumann solution which gives $s_t \rightarrow \infty$ as $t \rightarrow 0$.

Now, back-substituting $\xi = x/s(t)$ in (21) and using (19) we obtain an initial size and temperature profile for the solid phase at some small time $t > 0$, which we use to initialise our numerical scheme. We note by passing that defining $\sqrt{\lambda_2}/2 = \lambda$ the transcendental equation (22) becomes equal to that in (8).

5 Results and discussion

In Figure 1 we compare the temperature (at different times) and the position of the solidification front by the large β perturbation solution (circles) with the numerical solution by finite differences (solid line), for $\beta = 20$ (panels (a)-(b)) and $\beta = 5$ (panels (c)-(d)). The perturbation and the numerical solution show excellent agreement, even for a relatively small Stefan number $\beta = 5$, thereby validating the accuracy of the numerical solution.

Along with the (numerical and perturbation) solution to the Stefan problem with variable thermal conductivity we plot the Neumann solution to the classical problem (7)-(8) (dash-dotted line). By comparing the two, we observe that the overall effect of the size-dependent thermal conductivity on the solidification process is to delay the propagation of the temperature and the solidification front. Indeed, the delay is caused by a low value of the thermal conductivity $2s(\sqrt{s^2 + 1} - s)$ in the early stages of the solidification process when $s \approx \mathcal{O}(1)$. However, $k(t)$ quickly saturates to the maximum value of 1 (for instance, $s \approx 2$ already gives $2s(\sqrt{s^2 + 1} - s) \approx 0.95$) and the solution to the SP (6a)-(6e) converges to the Neumann solution. This is further illustrated in Figure 2.

In Figure 2 we show the position (left panel) and velocity (right panel) of the solidification front spanning several orders of magnitude in time for the case $\beta = 5$. The solution of the SP with size-dependent thermal conductivity (for clarity we

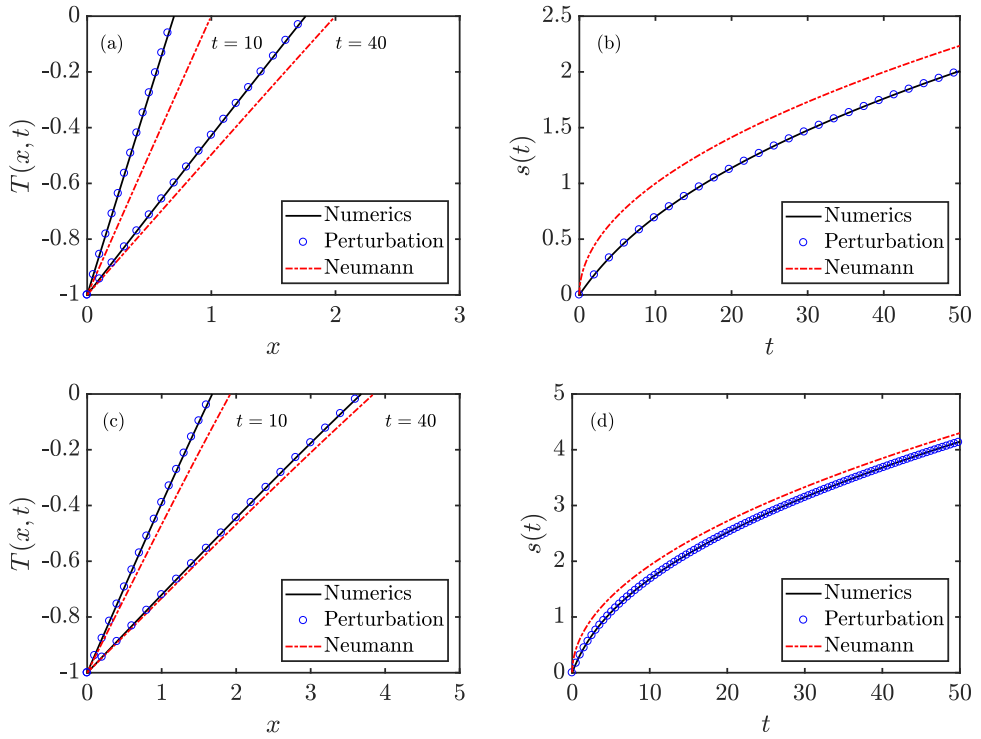


Figure 1: Temperature profiles at different times and position of the solidification front for the Stefan problem with size-dependent thermal conductivity and the standard Stefan problem. The circles, the solid line and the dash-dotted line represent the perturbation, the numerical and the Neumann solution, respectively. Panels (a)-(b) correspond to $\beta = 20$ and (c)-(d) to $\beta = 5$.

only show the numerical solution), represented by the solid line, shows different qualitative behaviour for small and large times which can be clearly identified in the log-log plots. For small times, the position of the front behaves linearly with time (according to eq. (19)) which is represented by the dashed line which has a slope 1. For large times, the position is well approximated by the Neumann solution, which is proportional to \sqrt{t} (according to eq. (8)), and so gives a slope of 0.5. The fact that $s \propto t$ as $t \rightarrow 0$ has an important physical implication, which is that the speed of the solidification front is constant and, thus, finite when solidification begins. In contrast, the Neumann solution gives $s_t \propto 1/\sqrt{t}$, leading to an infinite speed for the solidification front at the beginning of the process.

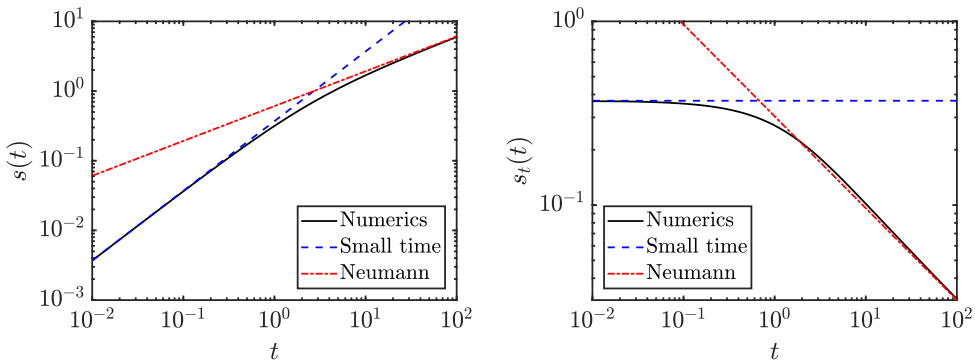


Figure 2: Position and velocity of the solidification front as a function of time spanning several orders of magnitude for the case $\beta = 5$. The solid line, the dashed line and the dash-dotted line represent the numerical, the small time asymptotic and the Neuman solution, respectively.

6 Conclusions

In this letter we have analysed a one-phase Stefan problem with size-dependent thermal conductivity. The problem has been solved numerically using an immobilisation transformation and a semi-implicit finite difference scheme. In addition, we have provided approximate analytical solution for large Stefan number and an asymptotic solution for small times. The small time limit analysis has revealed that the speed the solidification front is constant as $t \rightarrow 0$, whereas the Neumann solution to the classical problem predicts an unrealistic infinite velocity as time goes to zero. This result is very relevant as it gives a physically realistic description of how solidification phenomena initiates. When the size of the solid phase is approximately order 1, the qualitative behaviour of the solution switches

to the standard \sqrt{t} proportionality and the solution to the problem tends to the Neumann solution.

References

- [1] V. Alexiades and A.D. Solomon. *Mathematical Modelling of Freezing and Melting Processes*. Hemisphere Publishing Corporation, 1st. edition, 1993.
- [2] F. X. Alvarez and D. Jou. Memory and nonlocal effects in heat transport: From diffusive to ballistic regimes. *Applied Physics Letters*, 90(8):083109, 2007.
- [3] J. M. Back, S. W. McCue, and T. J. Moroney. Including nonequilibrium interface kinetics in a continuum model for melting nanoscaled particles. *Scientific Reports*, 4:7066, 2014.
- [4] J. Crank. *Free and Moving Boundary Problems*. Oxford University Press, 1st. edition, 1996.
- [5] F Font, T G Myers, and S L Mitchell. A mathematical model for nanoparticle melting with density change. *Microfluidics and Nanofluidics*, 18(2):233–243, 2015.
- [6] F. Font and T.G. Myers. Spherically symmetric nanoparticle melting with a variable phase change temperature. *Journal of Nanoparticle Research*, 15(12):2086, 2013.
- [7] S.C. Gupta. *The Classical Stefan Problem*. Elsevier, 1st. edition, 2003.
- [8] J. M. Hill. *One-Dimensional Stefan Problems: An Introduction*. Longman Scientific & Technical, 1st. edition, 1987.
- [9] D. Jou, J. Casas-Vazquez, G. Lebon, and M. Grmela. A phenomenological scaling approach for heat transport in nano-systems. *Applied Mathematics Letters*, 18(8):963 – 967, 2005.
- [10] Scott W McCue, Bisheng Wu, and James M Hill. Classical two-phase stefan problem for spheres. *Proceedings of the Royal Society of London A: Mathematical, Physical and Engineering Sciences*, 464(2096):2055–2076, 2008.
- [11] S.L. Mitchell and M. Vynnycky. Finite-difference methods with increased accuracy and correct initialization for one-dimensional stefan problems. *Applied Mathematics and Computation*, 215(4):1609 – 1621, 2009.

- [12] L.I Rubinstein. *The Stefan Problem.* Translations of Mathematical Monographs Vol. 27, (Ame. Math. Soc.), 1st edition, 1971.
- [13] H. S. Carslaw and J.C. Jaeger. *Conduction of heat in solids.* Oxford University Press, 1st edition, 1973.
- [14] A. M. Wallman, J. R. King, and D. S. Riley. Asymptotic and numerical solutions for the two-dimensional solidification of a liquid half-space. *Proceedings of the Royal Society of London A: Mathematical, Physical and Engineering Sciences*, 453(1962):1397–1410, 1997.